CALPHAD: Computer Coupling of Phase Diagrams and Thermochemistry 87 (2024) 102761

Contents lists available at ScienceDirect

Calphad

journal homepage: www.elsevier.com/locate/calphad

Catastrophe theory and thermodynamic instability to predict congruent melting temperature of crystals

Marcello Merli [a], Costanza Bonadiman [b], Alessandro Pavese [c,*]

[a] Department of Earth and Sea Sciences (DiSTeM), University of Palermo, Via Archirafi 36, 90123, Palermo, Italy
[b] Physics and Earth Sciences Department – University of Ferrara, Via Saragat 1, 44100, Ferrara, Italy
[c] Earth Sciences Department – University of Turin, Via Valperga Caluso 35, 10100, Turin, Italy

ARTICLE INFO

Handling Editor: Prof. Z.K. Liu

Keywords:
Melting temperature
Catastrophe theory
Thermodynamic instability
halite
Stishovite
Mg-perovskite

ABSTRACT

Melting temperature (T_m) is a crucial physical property of solids and plays an important role in the characterization of materials. Therefore, the capacity to predict T_m is a relevant issue for solid state sciences. This investigation aims i) to provide a theoretical basis for the link between catastrophe theory and thermodynamic instability; ii) to estimate T_m through the notion of "degenerate critical temperature" (T_d), related to (P_d,V_d,T_d), where $K_T \rightarrow 0$ and the Gibbs function shows a *non*-Morse behaviour; iii) to compare predictions of (P_m,T_m) with observations for three crystalline pure substances that undergo congruent melting and exhibit different bonding and stability ranges: NaCl (halite), $SiO_{2,st}$ (stishovite), and $MgSiO_3$ (perovskite). The *P-T locus* of $K_T = 0$ associated with melting is identified using the maximum values of T_d and $\Delta H/\Delta V$ at a given pressure. We observed an average absolute discrepancy ranging between 0.2 % (halite) and 5.8 % (stishovite), and an agreement between theoretical and experimental $T(P)_{melting}$-points from better than 1 to approximately 14 %.

1. Introduction

The catastrophe theory (CT), originally introduced by Thom [1] in the wake of Morse's work [2] and then formally systematized by Arnol'd [3], lends itself well to a variety of applications. In particular, to those in which a system becomes unstable upon an external perturbation, as summarized in the reference paper by Stewart [4] and in the successive book by Poston and Stewart [5]. CT pivots around the notion of "*degenerate critical*" points of a function, $\Phi(\boldsymbol{x};\boldsymbol{p})$: $R^n \times R^m \rightarrow R$, which describes the behavior of a system and depends on *n*-variables of state ($\boldsymbol{x}$), and *m*-control parameters ($\boldsymbol{p}$). A *critical* point ($\boldsymbol{x}_c$) of Φ is characterized by

$$\nabla\Phi(\boldsymbol{x}_c;\boldsymbol{p}) = 0. \quad (1)$$

If

$$\det\left[\left(\frac{\partial^2\Phi}{\partial x_i \partial x_j}\right)_{\boldsymbol{x}_c;\,\boldsymbol{p}}\right] \neq 0, \quad (2)$$

Φ is called *non*-degenerate at $\boldsymbol{x}_c$ (even termed "Morse function"), fulfils the Morse lemma, and by a change of variable, that is, $y_i = y_i(\boldsymbol{x};\boldsymbol{p})$, can be cast in the proximity of $\boldsymbol{x}_c$ as

$$\Phi(\boldsymbol{x};\boldsymbol{p}) - \Phi(\boldsymbol{x}_c;\boldsymbol{p}) = -\sum_{j=1}^{l} y_j^2(\boldsymbol{x};\boldsymbol{p}) + \sum_{k=l+1}^{n} y_k^2(\boldsymbol{x};\boldsymbol{p}). \quad (3)$$

Conversely, Φ is defined as *degenerate critical* at $\boldsymbol{x}_d$ (even called "*non*-Morse") if

$$\nabla\Phi(\boldsymbol{x}_d;\boldsymbol{p}) = 0 \quad (4)$$

and

$$\det\left[\left(\frac{\partial^2\Phi}{\partial x_i \partial x_j}\right)_{\boldsymbol{x}_d;\,\boldsymbol{p}}\right] = 0. \quad (5)$$

In this case, the state variables can be split into two sets: $\boldsymbol{x'} = (x'_1,\ldots, x'_l)$ and $\boldsymbol{x''} = (x''_{l+1},\ldots, x''_n)$, such that

$$\det\left[\left(\frac{\partial^2\Phi}{\partial x'_i \partial x'_j}\right)_{\boldsymbol{x}_d;\,\boldsymbol{p}}\right] \neq 0. \quad (6)$$

Φ is expressed around ($\boldsymbol{x}_d$; $\boldsymbol{p}$) by the linear combination of a Morse-type function and a *non*-Morse-type term (*NM*) using $\boldsymbol{x''}$:

$$\Phi = \sum_{j=1}^{l} \pm x'^2_j(\boldsymbol{x''};\boldsymbol{p}) + NM(\boldsymbol{x''};\boldsymbol{p}). \quad (7)$$

* Corresponding author.
E-mail address: alessandro.pavese@unito.it (A. Pavese).

https://doi.org/10.1016/j.calphad.2024.102761
Received 18 June 2024; Received in revised form 20 October 2024; Accepted 20 October 2024
Available online 4 November 2024

NM, in turn, is classified according to the scheme of the "catastrophe types" by Arnol'd [3]. Φ abruptly changes its behavior as a function of even small variations in the control parameters, thus causing the instability of the system. From this perspective, CT can indicate changes of state and phase transitions. Merli and Pavese [6] resorted to CT to predict instability that induces a transformation in crystals, exploiting an analysis of the degenerate critical points of the electron density. The same authors [7] investigated the relationship between melting and thermo-elastic anomalies involving the isothermal bulk modulus (K_T), which tends to vanish at given *P-T* values, using an approach that relies on classic thermodynamics and also considers the possibility of relating such a traditional strategy to CT.

The melting temperature (T_m) of crystals is integral to a wide range of scientific, technological, and industrial applications, impacting fields as diverse as materials science, chemistry, geology, physics, and energy. Notwithstanding that predicting T_m is an important issue, it is difficult to model this change of state, as reported by de With [8] and Gharakhanyan et al. [9]. Melting itself is an extremely complex phenomenon that takes place through a combination of factors, from surface (if dominant, then it is said "thermodynamic" melting) to bulk (in which case, "mechanical melting"), and involving defects that can either affect T_m or provide the very mechanism underlying the change of state. The review by de With [8] provides an exhaustive description of the state of the art; here, we mention a few of the more than 700 references cited therein. From a strictly thermodynamic point of view, melting requires a comparison between solid and liquid phases. Graeme et al. [10] formulated a two-state model that relied on the Gibbs energies of the solid and liquid phases to calculate T_m and its related Clapeyron slope. Techniques that resort to molecular dynamics have been proposed to predict the melting temperature [11], including the Z-method [12,13], two-phase method [14], and coexistence method [15]. Chakravarty and Lynden-Bell [16] combined the Landau theory with molecular dynamics and the Monte Carlo technique, while Trachenko [17] proposed a two-phase theory for melting, starting from the Clausius-Clapeyron equation and using a key representation of the energy of the liquid. However, the general difficulty in formulating a Gibbs energy model for liquids led scientists to consider one-phase approaches, which are oriented towards correlating the trend of particular observables with the occurrence of "critical" conditions that trigger instability in a solid phase. The collapse of the crystal structure was associated by Lindemann [18] and Gilvarry [19] with the average atomic oscillations becoming so large as to cause the superposition of one atom with another; this microscopic description, reformulated through the criterion of Guinea et al. [20], is consistent with the thermodynamic laws, as pointed out by Stacey and Irvine [21], and is suitable for atomistic modelling (see, for instance, Zhang et al. [22], about atomic motion in Cu-film melting). Herzfeld and Goeppert Mayer [23], Born [24], Ida [25], Boyer [26], Owens [27] and Digilov and Abramovich [28] underlined the relationship between thermoelastic ("lattice") instability and melting, focusing on the anomalies in the trend of observables such as volume thermal expansion, compressibility and/or shear modulus (elastic constants).

Based on the extant literature, we believe that the deep relationship between i) CT and ii) fundamental thermodynamic inequalities, which drive the transformations of a system, has hitherto been little explored and used, and a definite theoretical framework, wherein catastrophe theory and thermoelastic (lattice) instability meet, is still missing, to the best of our knowledge. Therefore, the aim of the present work is to demonstrate such a connection, and exploit it for the prediction of the melting temperature of pure crystalline 3D-substances that melt congruently. This was realized by seeking "*degenerate* critical pressure-temperature" values, $(P,T)_d$, that were associated with the notion of "*degenerate* critical points" of a thermoelastic observable (in the present case, isothermal bulk modulus: K_T), which ceases to be a Morse function at $(P,T)_d$. It is possible to design such a transformation that leads to a thermodynamic inequality violation, thus blocking a phase from existing as it is at $(P,T)_d$, and beyond. The couple $(P,T)_d$, in turn, is proposed as to be an estimate of $(P,T)_m$, under particular conditions that are related to T_d and to the change in enthalpy-over-volume ($\Delta H/\Delta V$) occurring in the associated reaction. The present work shows the connection between CT and thermodynamics, examines the topology of the $K_T = 0$ *locus*, and then focuses on case studies, for comparison with experiments from the literature, resorting to three minerals that exhibit different bonding types, crystal structures, and *P-T* ranges of stability: halite (NaCl), stishovite ($SiO_{2,st}$), and Mg-perovskite ($MgSiO_3$). Halite was modelled by quantum mechanics, accounting for thermal contribution by the Debye model with the addition of anharmonic effects; stishovite and Mg-perovskite were investigated using parametric and semi-empirical models formulated to represent their *P-V-T* Equations of State (EoSs). For each mineral, the calculated $(P,T)_d$ curves were compared with the observed $(P,T)_m$. With respect to Merli and Pavese [7], the present study provides the original background to consolidate and rationalize the use of K_T as an indication for incipient melting in a unifying theoretical framework. This was accomplished through: i) a synergic approach that combines CT and thermodynamics; ii) the definite proof that $K_T = 0$ is a condition of *non*-existence for a solid because of the implication relating to a thermodynamic inequality violation, independently of the order of expansion of the Gibbs potential; iii) the employment of the $K_T = 0$ *P-T locus* to locate univocally the curve candidate to represent melting; iv) three case studies that cover not only bonding types from ionic to ionic-covalent, but also provide totally different approaches to determine the $K_T = 0$ *locus*.

The present investigation can provide an added-value to the current knowledge about modelling T_m, at least in two respects:

1) although $K_T = 0$ provides a condition associated with the general instability of systems (melting is a particular case that can be univocally identified among the transformations predicted) that has already been proposed by a variety of Authors (see de With [8] for a survey), a full theoretical justification, which conjugates physical and "universal" mathematical aspects, is still lacking, to the best of our knowledge;
2) catastrophe theory is a powerful instrument underused in research. CT cannot provide a physical explanation of the collapse that is forecast, yet it provides a very general scheme that, relying only on mathematical features of the function describing a phenomenon, or a physical property, signals an incipient transformation. In the light of this, it can be noted that CT, even alone, points to the occurrence of the conditions, which include melting, heralding a structure collapse. The established general physical link between degenerate critical points and thermodynamic inequality violation, explained in the text that follows, has a "universal" character. Hence, such an aspect might be considered in relation to varieties of phenomenology, even other than melting, utilising CT and its comparative simplicity of application, which reduces to the analysis of first/second derivatives.

The present investigation is one of the few in which catastrophe theory is employed to investigate the transformations of solids, resorting to "mechanical" instability as a consolidated link to a physical condition that in turn leads to the impossibility for a system to preserve itself beyond a given $(P,T)_d$.

2. Theoretical methods

2.1. Catastrophe theory and thermodynamics

We investigated the conditions that mark the transformation of a crystal by combining CT and fundamental thermodynamic theorems. The method of Callen (1960) [29] was adopted to describe a solid system that becomes mechanically unstable starting from an equilibrium point (P,V,T). The system was split into two subsystems, both of mass $M_{tot}/2$, and their volume was changed by infinitesimal amounts $\pm\delta V$. The

pressure (P) and temperature (T) of the thermo-barostat are preserved so that (P,$V/2+\delta V$,T) and (P,$V/2-\delta V$,T), with densities of $M_{tot}/(V+2\delta V)$ and $M_{tot}/(V-2\delta V)$, respectively, are the thermodynamic coordinates of the subsystems *out of equilibrium*. The subsystems undergo an internal re-equilibration at a given (P,T), passing from (P,$V/2+\delta V$,T) + (P,$V/2-\delta V$,T) to (P,$V/2$,T) + (P,$V/2$,T), that is, $\delta V \to 0$. Such a transformation, which occurs spontaneously, is likened to an *irreversible* "real process". Please, note that the *total* system, which is composed of the two subsystems defined above, preserves its volume as $V = (V/2+\delta V) + (V/2-\delta V)$ upon equilibration with pressure and temperature of the thermo-barostat. The Gibbs energy change taking place in the irreversible equilibration can be calculated as follows:

$$\begin{aligned}\Delta G(\delta V;P,V,T)_{irrev} &= 2\times G(P,V/2,T) - \left[G\left(P,\frac{V}{2}+\delta V,T\right)+G\left(P,\frac{V}{2}-\delta V,T\right)\right] = G(P,V,T) - \left[G\left(P,\frac{V}{2}+\delta V,T\right)+G\left(P,\frac{V}{2}-\delta V,T\right)\right]\\ &= = F(V,T)+P\times V - \left[F\left(\frac{V}{2}+\delta V,T\right)+P\times\left(\frac{V}{2}+\delta V\right)+F\left(\frac{V}{2}-\delta V,T\right)+P\times\left(\frac{V}{2}-\delta V\right)\right] = F(V,T) - F\left(\frac{V}{2}+\delta V,T\right) - F\left(\frac{V}{2}-\delta V,T\right)\\ &= F(V,T) - F\left[\frac{1}{2}\times(V+2\delta V),T\right] - F\left[\frac{1}{2}\times(V-2\delta V),T\right] = F(V,T) - \frac{1}{2}[F(V+2\delta V,T)+F(V-2\delta V,T)]\end{aligned} \tag{8}$$

In (8), the first-degree homogeneity of the Helmholtz/Gibbs potentials with respect to volume at a given density was exploited. *P-V-T* can be likened to control parameters, whereas δV is treated as a state variable describing the deviation from equilibrium and whose evolution is associated with re-equilibration. An alternative route is possible using the little employed but elegant notion of *availability*, which can formalize how equilibration occurs between a system, forced out of equilibrium, and its surroundings. Using the Taylor expansion of the two terms between square brackets in the last member of (8), and replacing $2\delta V$ with Δ, for simplicity of notation, it is obtained:

$$\Delta G(\Delta;P,V,T)_{irrev} = -\frac{1}{2}\left[\sum_{n=1}^{\infty}\frac{1}{n!}\left(\frac{\partial^n F}{\partial V^n}\right)_T\times(1+(-1)^n)\times\Delta^n\right] \tag{9}$$

that can be readily recast into

$$\Delta G(\Delta;\ P,V,T)_{irrev} = -\left[\sum_{n=1}^{\infty}\frac{1}{2n!}\left(\frac{\partial^{2n}F}{\partial V^{2n}}\right)_T\times\Delta^{2n}\right] \tag{10}$$

where $m! = m\times(m-1)\ldots\times 1$. Eq. (10) shows that ΔG_{irrev} is a function of the off-equilibrium shift (Δ) only, and its derivatives at $\Delta = 0$ are such that

$$\left(\frac{\partial^{2n+1}\Delta G_{irrev}}{\partial\Delta^{2n+1}}\right) = 0 \tag{11}$$

and

$$\left(\frac{\partial^{2n}\Delta G_{irrev}}{\partial\Delta^{2n}}\right) = -\left(\frac{\partial^{2n}F}{\partial V^{2n}}\right)_T. \tag{12}$$

$\Delta G(\Delta;P,V,T)_{irrev}$ is intrinsically "*critical*" at $\Delta = 0$, that is, (P,V,T), because of (11), and exhibits a behaviour around (0; P,V,T), which depends only on the even derivatives of the Helmholtz energy.

Irreversible transformations fulfil for any Δ the well-established thermodynamic inequality that follows

$$\Delta G(\Delta;\ P,V,T)_{irrev} < 0. \tag{13}$$

Writing ΔG_{irrev} in terms of the expansion beneath:

$$\Delta G(\Delta;\ P,V,T)_{irrev} = \sum_{n=1}^{\infty}\Delta G(\Delta;\ P,V,T)^{2n}_{irrev} \tag{14}$$

and dropping (Δ; P, V, T) for simplicity, yields:

$$\Delta G^2_{irrev} = -\frac{1}{2!}\left(\frac{K_T}{V}\right)\Delta^2 \tag{15}$$

$$\Delta G^4_{irrev} = -\frac{1}{4!}\left[\frac{2}{V^3}K_T - \frac{2}{V^2}\left(\frac{\partial K_T}{\partial V}\right)_T + \frac{1}{V}\left(\frac{\partial^2 K_T}{\partial V^2}\right)_T\right]\Delta^4 \tag{16}$$

$$\Delta G^{2n}_{irrev} = -\frac{1}{2n!}\frac{1}{V}\left[\sum_{l=0}^{2n-2}\frac{C_l}{V^{2n-2-l}}\times\left(\frac{\partial^l K_T}{\partial V^l}\right)_T\right]\Delta^{2n}. \tag{17}$$

The nth-order volume derivative of the isothermal bulk modulus (in thermodynamic coordinates *V-T*) can be expressed as follows:

$$K^n = \left(\frac{\partial^n K}{\partial V^n}\right)_T \tag{18}$$

assuming that

$$K^0 = \left(\frac{\partial^0 K_T}{\partial V^0}\right)_T = K_T. \tag{19}$$

It follows that

$$dK^n = \left(\frac{\partial K^n}{\partial V}\right)_T dV + \left(\frac{\partial K^n}{\partial T}\right)_V dT\,. \tag{20}$$

If the thermodynamic coordinates *P-T* are introduced in place of *V-T* to express the differentials, then Eq. (20) becomes

$$dK^n = \left(\frac{\partial K^n}{\partial V}\right)_T\times\left[\left(\frac{\partial V}{\partial P}\right)_T dP + \left(\frac{\partial V}{\partial T}\right)_P dT\right] + \left(\frac{\partial K^n}{\partial T}\right)_V dT, \tag{21}$$

and setting isothermal conditions, that is $dT = 0$, we obtain

$$\left(\frac{\partial K^n}{\partial P}\right)_T = -\left(\frac{\partial K^n}{\partial V}\right)_T\times\frac{V}{K_T}, \tag{22}$$

which can be rearranged into

$$\left(\frac{\partial K^n}{\partial V}\right)_T = -\frac{K_T}{V}\left(\frac{\partial K^n}{\partial P}\right)_T. \tag{23}$$

In the case of $K_T = 0$, occurring at (P_d,V_d,T_d) = (P,V,T)$_d$, $\Delta G(\Delta;\ P_d, V_d, T_d)_{irrev}$ becomes "*degenerate critical*", such as to engender a *catastrophe* behaviour of "cuspoid" type, as labelled with $A_{m\geq 4}$ in Ref. [30], because of (15). Moreover, Eq. (23) in combination with Eq. (17) yields

$$\Delta G(\Delta;\ P_d, V_d, T_d)_{irrev} = 0, \tag{24}$$

which implies a violation of thermodynamic inequality (13) at any order

in Δ. Moreover, Eq. (24) indicates that (P_d,V_d,T_d) and $(P_d,V_d/2+\delta V,T_d)$ + $(P_d,V_d/2\text{-}\delta V,T_d)$ have the same *G*-energy, which conflicts with the fact that the former is a point of equilibrium where the system can remain indefinitely, whereas the latter is an off-equilibrium, such that re-equilibration occurs spontaneously. This proves the impossibility of a system to undergo irreversible equilibration to $(P,V,T)_d$ from an off-equilibrium point, as expressed by the shift in the fundamental thermodynamic *V*-coordinate. In the light of this, *non*-Morse conditions and thermodynamic inequality violations are strictly related to one another at $K_T \to 0$, which indicates that a system cannot exist as it is and therefore needs a transformation into a more stable unknown new phase. Moreover, choosing a (P,T) point in the stability region of the crystal, i.e. $P = P_d + \Delta P$ and $T = T_d + \Delta T$ ($\Delta T < 0$; $\lim_{T\to T_d} T_d - T = 0^+$), and taking Eq. (24) into account, ΔG_{irrev} can be written in terms of a generalized factorization (see the analogy with Landau expansion; Tolédano and Tolédano [31]), as follows:

$$\Delta G(\Delta;\ P,V,T)_{irrev} = \left[A(T_d - T)^{\beta} + B|P_d - P|^{\alpha}\right] \times f(\Delta;\ P,V,T) \tag{25}$$

where *A*, *B*, β and $\alpha > 0$; *f* is a function such that $f(P,V,T;\ \Delta) < 0$ for ΔG_{irrev} to satisfy (13) at $(P,V,T) \neq (P,V,T)_d$. The change in entropy due to irreversible transformation is determined by

$$\Delta S(\Delta;\ P,V,T)_{irrev} = -\frac{\partial \Delta G(\Delta;\ P,V,T)_{irrev}}{\partial T} \ . \tag{26}$$

In Eq. (26), the following possibilities occur:

$0 < \beta < 1$ giving $\lim_{(P,T)\to(P,T)_d} \Delta S(\Delta;\ P,V,T)_{irrev} = -\infty$,

$\beta = 1$ giving $\lim_{(P,T)\to(P,T)_d} \Delta S(\Delta;\ P,V,T)_{irrev} = f(\Delta;\ V_d,T_d,P_d) < 0$,

$\beta > 1$ giving $\lim_{(P,T)\to(P,T)_d} \Delta S(\Delta;\ P,V,T)_{irrev} = 0$

Using the first law of thermodynamics for an infinitesimal re-equilibration of type $(P,V/2+\delta V,T) + (P,V/2 - \delta V,T) \to (P,V/2,T) + (P,V/2,T)$, yields:

$$\delta Q = U(V,T) - \left[U\left(\frac{V}{2}+\delta V,T\right) + U\left(\frac{V}{2}-\delta V,T\right)\right] + P\delta V - P\delta V = 0. \tag{27}$$

Therefore, taking $dS_{irrev} > \delta Q/T$ into account, for an irreversible transformation like that in (27), it holds that

$$\Delta S(\Delta;\ P,V,T)_{irrev} > 0. \tag{28}$$

This condition contrasts with the fact that the change in entropy determined using Eq. (25) implies

$$\lim_{(P,T)\to(P,T)_d} \Delta S(\Delta;\ P,V,T)_{irrev} \leq 0 \tag{29}$$

2.2. *P-T* melting curve

The *locus* of *P-T* such that $K_T = 0$, that is, $(P,T)_d$, is provided by the following curve:

$$\Phi(P_d,T_d;K_T = 0) = 0\ . \tag{30}$$

Eq. (30) can be reconsidered in the frame of the *P-V-T* equation of state associated with a crystal, in combination with the constraint $K_T = 0$:

$$P = EoS(V,T) \tag{31}$$

$$\left(\frac{\partial P}{\partial V}\right)_T = 0 \tag{32}$$

The equations above yield the 1D-manifolds announcing instability, including the one associated with the estimate of the *P-T* melting curve.

Two $(P,T)_d$ points, infinitesimally close to one another and belonging to Φ, are such that

$$\delta\Phi = \left(\frac{\partial\Phi}{\partial P}\right)_T \delta P + \left(\frac{\partial\Phi}{\partial T}\right)_P \delta T = \Phi_P \delta P + \Phi_T \delta T = 0 \tag{33}$$

because of (30).

Therefore, from (33) it ensues

$$-\frac{\Phi_T}{\Phi_P} = \Phi' = \frac{\delta P}{\delta T}. \tag{34}$$

Using Eq. (34), Φ can be linked to a physical quantity *via* the Clapeyron equation, that is,

$$-\Phi' = \frac{\Delta S}{\Delta V} \tag{35}$$

where ΔS and ΔV are the differences in molar entropy and volume, respectively, between the phases at equilibrium along the transformation curve. The condition $\Phi' \neq 0$, owing to Eq. (34), implies that the implicit function of *P-T* given by Eq. (30) is invertible, such that the degenerate pressure and temperature values are related to one another in terms of

$T_d = T(P_d)$

and

$P_d = P(T_d)$.

Moreover, the *P-T* regions that are.

(i) located where Eq. (30) provides differentiable manifolds (i.e., *P-T* ranges, where Φ is continuous and $\Phi' \neq 0$);
(ii) disjointed from each other (i.e. exhibiting discontinuities between each other),

allow the determination of different $T_d = T(P_d)$ curves, each of which refers to a given type of "criticality", announcing the need of a highly probable readjustment of the system.

Eq. (35) can be recast as follows

$$-\Phi' \times T_d = \frac{\Delta H}{\Delta V} \tag{36}$$

where ΔH is the enthalpy change during the transformation at T_d and is related to the exchanged heat ΔQ.

All this suggests that among the criticalities pointed out by a vanishing K_T there is the melting transition of state, too. In such case, melting is the transformation accompanied by the largest values of T_d (at a given pressure) and $\Delta H/\Delta V$ in crystals undergoing congruent fusion, as shown in Ref. [32]. Moreover, $\Delta V = V_{liquid} - V_{solid}$ is commonly positive (and $\Delta H/\Delta V$ likewise), with $\Delta V/V_{solid}$ values in the range of 4–20 % [8], save for a few exceptions such as Si, Ge, Bi, and H_2O [8,33,34]. In the case of $\Delta V < 0$, the conditions stated above are preserved by taking the absolute value of $\Delta H/\Delta V$.

Therefore, the *locus* defined in Eq. (30) and associated with the largest (absolute) values of Eq. (36), and T_d (for a given pressure) locate the chosen curve as the likeliest candidate to represent the congruent melting of a crystalline substance.

2.3. *About the nature of $K_T(P_d,T_d) = 0$*

It is important to provide a more solid classification of the nature of the phenomenon associated with a vanishing K_T. An infinitesimal change of the Gibbs energy of an irreversible transformation [35,36] can be written as

$$dG_{irrev} = VdP - SdT + \sum_{j=1,N}\mu_j dn_j - TdS_{irrev}$$
$$= VdP - SdT + \sum_{j=1,N}\mu_j dn_j - Dd\varepsilon + \frac{1}{2}D_2 d\varepsilon^2 - \frac{1}{6}D_3 d\varepsilon^3 \quad (37)$$

where dS_{irrev} is the part of entropy related to an irreversible transformation and therefore >0; $d\varepsilon$ provides a measure of the degree of progress of the transformation; the coefficients "D" represent the Taylor expansion of TdS_{irrev} and must fulfil the condition of production of entropy in addition to $\delta Q/T$ in an irreversible process. In the case of a pure substance (closed and unreactive system) undergoing an isobaric-isothermal irreversible transformation towards equilibration, then

$$dG_{irrev} = -Dd\varepsilon + \frac{1}{2}D_2 d\varepsilon^2 - \frac{1}{6}D_3 d\varepsilon^3 < 0 \quad (38)$$

If $D = 0$ equilibrium is achieved, which can be "stable" ($D_2>$) or "unstable" ($D_2 < 0$). $D_2 = 0$ corresponds to the "*limit of stability*", and when also $D_3 = 0$, this becomes a "*critical point*". Adopting such a classification and terminology for the case ($d\varepsilon = \delta V$), $K_T = 0$ is referred to as a critical (P,T)-point. Please note that the appearance of "instability", in terms of "limit of stability" and "unstable equilibrium", is related to a condition involving one phase only, and indicating an incipient transformation. In the light of this, it is important to distinguish such a situation from that of a "phase transition" *tout-court*, which takes place by overcoming a potential barrier through thermal fluctuations.

2.4. Melting phenomenology

A question is whether

$$\lim_{(P,T)\to(P,T)_d} K_T = 0 \quad (39)$$

invariably provides an estimate of T_m *via* T_d. As discussed above, a vanishing K_T is related to both an incipient catastrophe and thermodynamic violation, thus showing that the system is expected to undergo a fluctuation given that it cannot preserve itself as it is. The changes in volume, pressure, and temperature along the solid-melt equilibrium curve can be written in terms of

$$\delta V = \left[\left(\frac{\partial V}{\partial T}\right)_P \delta T + \left(\frac{\partial V}{\partial P}\right)_T \delta P\right] \quad (40)$$

and therefrom

$$\frac{\delta V}{\delta T} = \left[\left(\frac{\partial V}{\partial T}\right)_P + \left(\frac{\partial V}{\partial P}\right)_T \frac{\delta P}{\delta T}\right]. \quad (41)$$

Following Boyer [26], the left-hand-side of the above relationship is negligible with respect to that of the right-hand side. Therefore, Eq. (41) can be rewritten as follows:

$$\frac{\delta P}{\delta T} = K_T \alpha \quad (42)$$

where α is the bulk thermal expansion coefficient. Boyer [26], on the basis of a thorough analysis of the extant literature and using both observations and results from modelling, claimed that melting ought to be related to the occurrence of thermoelastic instability, which, in turn, is connected to a divergence of the volume thermal expansion, that is,

$$\lim_{T\to T_m} \alpha = \infty. \quad (43)$$

Table 1
Coefficients of equ.(45) for NaCl are set out, with their 95 % confidence ranges, where V(Bohr^3; crystallographic cell volume) and T(K). The parameters used to calculate equ.(47) according to the models by Wang et al. [48] and Aizawa and Yoneda [49] are reported, for stishovite and perovskite (for both the third order Birch EoS is employed for the static pressure; the crystallographic cell volume in Å^3 is used), respectively. Please, note that the Debye temperature is referred to by Refs. [48,49] using Θ_D/θ, in place of T_D as here; T_{D0} = Debye temperature at room conditions. $ From O.L. Anderson, Thermoelastic properties of $MgSiO_3$ perovskite using the Debye approach, Am. Mineral. 83 23–35 (1998).

	NaCl	$SiO_{2,st}$		$MgSiO_3$	
p_{00}	3.024 (2.49, 3.558)	V_0(Å^3)	46.55	V_0(Å^3)	162.3
p_{10}	1.180 (−2.082, 4.441)	K_{T0}(GPa)	294	K_{T0}(GPa)	261
p_{01}	−1.300 (−5.314, 2.713)	K'	4.85	K'	4
p_{20}	1.681 (−5.019, 8.381)	T_{D0}(K)	1130	T_{D0}(K)	1076$^{\$}$
p_{11}	3.570 (−12.19, 19.33)	γ_0	1.66	γ_0	1.43
p_{02}	2.197 (−6.331, 10.72)	A	1	q	2.1
p_{30}	−1.023 (−6.218, 4.172)	B	2.9		
p_{21}	−4.133 (−21.55, 13.28)				
p_{12}	−4.642 (−21.95, 12.67)				
p_{03}	−1.183 (−5.385, 3.019)				

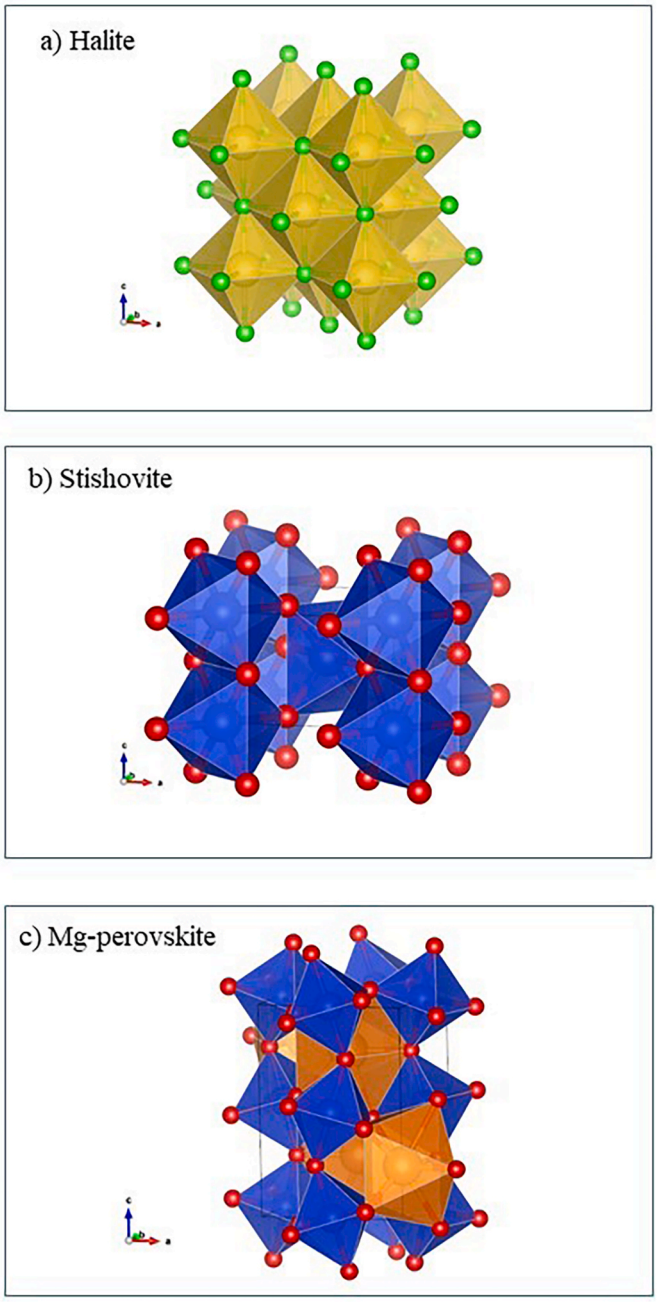

Fig. 1. Crystal structures of the minerals used as case studies, described through coordination polyhedra. (**a**) NaCl (halite) structure; yellow = sixfold $NaCl_6$ polyhedra. (**b**) $SiO_{2,st}$ (stishovite) stucture; blue = sixfold SiO_6 polyhedra. (**c**) $MgSiO_3$ (Mg-Perovskite) structure; orange = twelvefold MgO_{12} polyhedra; blue = sixfold SiO_6 polyhedra.

Dating back to the 30s, the same conclusion was reached by Herzfeld and Goeppert Mayer [24] who, on the basis of an elementary Debye-like model and available experimental data, maintained that the compressibility of a crystal at its melting point tends to infinity, as well as thermal expansion (see Eq. (30) in the aforementioned study). In a review by Drebushchak [37] the current theories underlying thermal expansion are discussed in the light of experimental data. The cited Author mentions and considers explicitly the "anomalous" behaviour at high temperature of α that tends to diverge in proximity of melting. Such a trend may be differently motivated and modelled, but its recognition is shared by those authors, who deal with the metric change in solids upon heating. Most of the substances analysed are crystalline solids and for such materials Eqs. (42) and (43) can be combined, so that Eq. (39) is expected to be reasonably useable as a signal, indicating the physical onset of the conditions leading to melting. Notwithstanding this, i) to the best of our knowledge, no theoretical absolute motivation exists to claim the validity of Eq. (43) as a constraint for any solid at its congruent melting point; ii) $K_T \rightarrow 0$ holds even in relation to transformations other than melting, and involves lower T_d and smaller $\Delta H/\Delta V$. In fact, the vanishing of the isothermal bulk modulus as a limit condition associated with a solid-to-solid transformation was precisely measured; for instance, Angel et al. [38] and McConnell et al. [39] used the Landau expansion as a function of the order parameter, in terms of a customary approach, to treat group-subgroup and incommensurate transitions, respectively.

Digilov and Abramovich [28] related melting to thermal pressure, achieving a critical value as large as $K_T = {}_0/(\delta_T \times e)$ in combination with an isothermal bulk modulus $K_{Tm} = K_{T=0}/e$ (δ_T is the Anderson-Grüneisen parameter). This model relies on a perfectly quasi-harmonic solid and exploits the Debye model to calculate the thermal energy; such an approximation is expected to lack precision in the proximity of a change of state, where anharmonicity becomes relevant. Merli and Pavese [7] performed quantum mechanics calculations complemented by lattice dynamics to account for the thermal contribution, in the case of MgO (periclase). The mentioned authors corrected their quasi-harmonic model by introducing an anharmonic contribution, which significantly improved the experimental-theoretical agreement by reducing the overestimation of T_m, the latter predicted *via* $K_T = 0$. A decrease in the estimated T_m would have been achieved by setting $K_T = K_{T=0}/e$ as a critical value for the isothermal bulk modulus, meanwhile preserving the quasi-harmonic model as a general framework for calculations. Please note that lattice dynamics generally provides more precise results than the Debye model, and in such respect an important difference occurs between the works reported in Refs. [7,28].

2.5. Computing

Calculations to determine the *P-T locus* of $K_T = 0$ were performed using two approaches. For NaCl (halite), a quantum model was developed using the HF/DFT-CRYSTAL17 program [40] that implements the strategy of the "Ab-initio Linear-Combination-of-Atomic-Orbitals" in crystals to construct basis sets that are then employed in a mixed Hartree-Fock/Density-Functional-Theory calculation scheme. The correlation energy was accounted for by a combination of the SOGGA functional (Second Order Generalized Gradient Approximation [41]) and PBE functional [41,42], using a hybridization rate of 20 %, which enabled the satisfactory reproduction of halite structures under room conditions (deviation within 0.1 %, in the case of the volume). The accuracy of the integrals that are involved in the self-consistent-field cycles were set at the following values: 10^{-8} C overlap; 10^{-8} C penetration, 10^{-8} exchange overlap; 10^{-8} exchange pseudo-overlap (direct space); 10^{-16} exchange pseudo-overlap (reciprocal space); 10^{-9} a.u. for SCF-cycle convergence. Outer shell exponents for Na and Cl were optimized by the "billy" utility [43]. The eigenvalue level shifting method (1.0 Ha) was employed to prevent possible conducting-state solutions and promote convergence. For sodium, the basis set Na_8–511(1d) G_baranek_2013_NaTaO3 was used [44], whereas Cl was modelled by Cl_86-311G_apra_1993 [45]. Minimization of enthalpy at 0 K was performed at nominal static pressure P_{st}, thus determining the related volume, V. The harmonic vibrational contribution to the Helmholtz energy (F) was calculated using the Debye model, employing Otero-de-la-Roza et al. [46] to determine T_D (Debye temperature) by means of V and the Poisson ratio from static simulations. An estimate of the uncertainty affecting the thermal contribution to energy ($E_{thermal}$) owing to the uncertainty on T_D is obtained by means of the propagation of errors. Using the Debye model yields

$$\frac{\Delta E_{thermal}}{E_{thermal}} = \frac{1}{E_{thermal}}\left(\frac{\partial E_{thermal}}{\partial T_D}\right) \times \Delta T_D = \frac{1}{E_{thermal}} \times C_V \times \left(\frac{T}{T_D}\right) \times \Delta T_D \approx \frac{1}{< C_V > \times T} \times C_V \times \left(\frac{T}{T_D}\right) \times \Delta T_D = \frac{C_V}{< C_V >} \times \frac{\Delta T_D}{T_D} \approx \sigma \frac{\Delta T_D}{T_D} \tag{44}$$

where $\sigma \gtrsim 1$, C_V is the constant volume specific heat capacity, and ΔT_D represents the uncertainty due to the approximation in estimating T_D. In the case of NaCl, a relative error of ~5 % was assumed, which reasonably propagates on P with the same magnitude. Using the $T_d = T(P_d)$ curve discussed in the ensuing section to estimate T_m, the uncertainty affecting P reflects on the calculated melting temperature in terms of an average error of ~6 K, i.e. a relative error of ~0.4 %. Such a relative error, on the one hand, is quasi-negligible, in view of the experimental uncertainty on the measurements of T_m, and, on the other hand, it is of the same magnitude as the discrepancy between observations and predictions, as it will be shown below.

The anharmonic contribution to F was accounted for by the Wu and Wentzcovich [47] model, whose "c" parameter was determined to estimate a T_D value equal to that obtained from the experiments under ambient conditions. In this work, $F(V,T)$ was calculated at 300 volume-temperature points, which allowed the obtainment of the Helmholtz function by interpolation using a polynomial in V-T up to the third order. The actual pressure was calculated as $-(\partial F/\partial V)_T$ and parametrized as a function of V and T in terms of

$$P = \sum_{j,k=0}^{j+k\leq 3} p_{jk} T^j V^k. \tag{45}$$

In the case of $SiO_{2,st}$, the parametric model of Wang et al. [48] based on the *P-V-T* Mie-Grüneisen equation of state fitted to X-ray powder diffraction data was employed to determine the *P-T locus* of $K_T = 0$. In particular, the pressure is split into the following two contributions:

$$P(V,T) = P_{300\ K} + \Delta P_{thermal}(V,T) \tag{46}$$

The first term of the right-hand side member was modelled using the classic Birch equation, whereas $\Delta P_{thermal}$ was accounted for by:

$$\Delta P_{thermal}(V,T) = \frac{\gamma(V)}{V}\left[E_{thermal}(V,T) - E_{thermal}(V,300K)\right] \tag{47}$$

resorting to the Debye model for thermal energy and to the parameterization reported by the aforementioned authors to express the Grüneisen parameter.

In the case of $MgSiO_3$ (perovskite), the *P-V-T* parameterization of Aizawa and Yoneda [49], whose model is close to the one described above, was used.

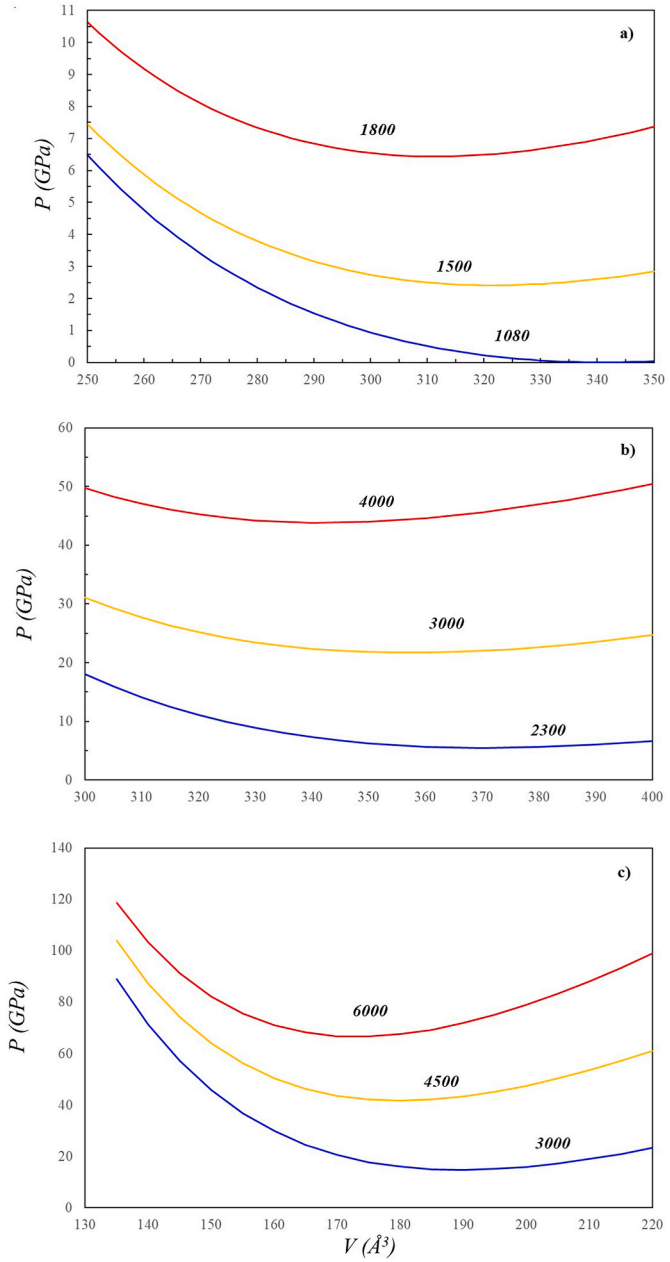

Fig. 2. *P-V* isothermal curves for halite (**a**), stishovite (**b**) and perovskite (**c**); the chosen isotherms of each mineral represent melting at comparatively low (blue), medium (yellow) and high (red) pressure with respect to the stability field resulting in experiments or observed in natural environments. The *T* values are reported in Kelvin (K). Degenerate critical points are determined by the location of the minima, where $(\partial P/\partial V)_T = 0$. Calculations were carried out as reported in "***Computing***". Note that for halite a quantum mechanical modelling was employed, whereas for stishovite and perovskite semi-empirical parametrizations of *P-V-T EoS* were used.

The *P-V-T* surfaces produced for halite, stishovite, and perovskite were analysed using MATLAB to locate the degenerate points given by

$$\left(\frac{\partial P}{\partial V}\right)_T = 0. \tag{48}$$

The manifold provided by Eq. (30), which maximizes Eq. (36) and T_d for a given pressure, was selected to obtain the *P-T* melting curve.

In Table 1 the parameters used for Eq. (43), in the case of NaCl, and to implement the model of equ.(45), in the case of $SiO_{2,st}$ and $MgSiO_3$, are reported.

3. Results and discussion

The crystal structures of halite (NaCl; SG: $Fm\bar{3}m$), stishovite ($SiO_{2,st}$; SG: $P4/mnm$), and perovskite ($MgSiO_3$; SG: *Pnma*) are shown in Fig. 1a-b-c. Relevant differences are appreciable in both the bonding and atomic arrangements. In the case of NaCl (quasi-fully ionic bonding), sodium and chlorine atoms alternately occupy sites located at the corners (Fig. 1a), half edges, centre of each face, and centre of the cubic cell, so that Na(Cl) assumes octahedral coordination. $SiO_{2,st}$ (ionic-covalent bonding) is isostructural to rutile, with silicon in unusual octahedral coordination (Fig. 1b) because of the high-pressure regime required to

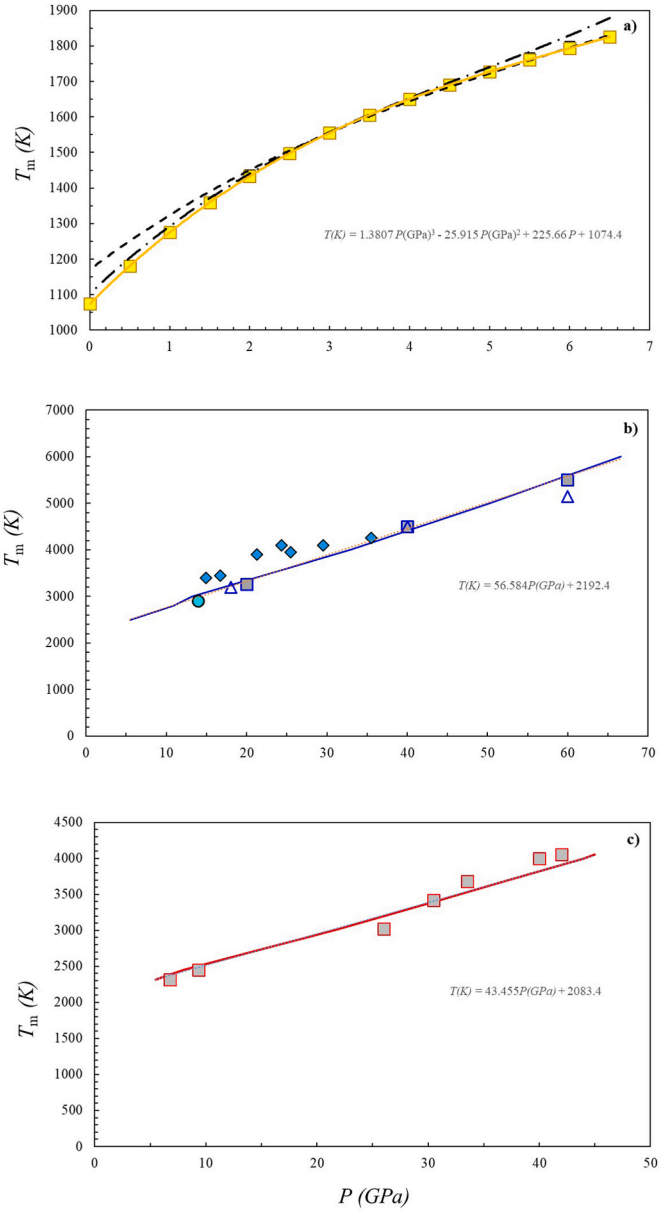

Fig. 3. Melting temperature (T_m estimated by T_d) as a function of pressure. *P-T* are determined as the *loci* of $K_T = 0$ for halite (**a**), stishovite (**b**) and Mg-perovskite (**c**). The solid lines represent the melting *P-T* curves from our estimates. In (**a**), the square symbols correspond to the observations of Akella et al. [50]; dashed-line/dot-dashed-line: Mie-Grüneisen/Birch EoS for determination of the *locus* of $K_T = 0$ corresponding to melting. In (**b**), diamonds are the experimental data by Shen and Lazor [58] the circle shows a measurement of Zhang et al. [59]; the squares refer to the modelling of Luo et al. [60]; triangles from Belonoshko and Dubrovinsky [52]. In (**c**), the squares stand for observations by Shen and Lazor [58].

stabilize such a phase. $MgSiO_3$ (bonding types with different degrees of ionic-covalent character) has Si dwelling in an octahedral site, and Mg exhibits cuboctahedral coordination (Fig. 1c); it is a high-pressure phase and a major constituent of the Earth's lower mantle. Fig. 2a-b-c report, as an example, three isothermal *V-P* curves that show how, for a given temperature and focusing on a comparatively narrow *V*-range, the $(P,V,T)_d$ points are determined through the constraint $(\partial P/\partial V)_T = 0$, using $P = -(\partial F/\partial V)_T$ in the case of halite and $P = EoS(V,T)$ for the others. As underlined by Ref. [7], an unphysical region occurs where an increase in *V* is associated with an increase in *P*, that is, $K_T < 0$ and therefore $dP_{lattice}/dV + dP_{vib}/dV > 0$. The failure of the energy model points out the impossibility to provide a physically sound representation beyond a given limit in the *P-T* space, in keeping with the violation of a fundamental thermodynamic inequality. The *V*-intervals displayed refer to those around the estimated melting volumes. The isotherms were chosen to represent melting at comparatively low, medium, and high pressures with respect to the stability field explored in the experiments or observed in natural environments for the phases involved. Halite stability is notably dependent on humidity (critical value 76 %), with an experimentally determined melting point at room pressure of ~1078 K [50] and boiling point of ~1738 K [51]. Therefore, the *V-P* curves of halite were chosen at 1080, 1500, and 1800 K. Experimental and theoretical studies have been reported for the T_m-figures of stishovite from ~2000 (at a minimum pressure of ~15 GPa [50]) up to ~8300 K [52,53]. The *V-P* melting curves of stishovite are displayed at 2300, 3000, and 4000 K, for them to cover a thermal range comparable to that of its natural occurrence. Based on the available experimental data and theoretical studies [54], the melting temperature of Mg-perovskite in the *P*-range referred to Earth's interiors, is 2800–8000 K. Thus, reference temperatures of 3000 K, 4500 K, and 6000 K were chosen in this study for the isothermal *V-P* curves of Mg-perovskite. The *P-T* melting curves estimated by the *loci* of $K_T = 0$ and the largest $\Delta H/\Delta V$ values are presented in Fig. 3a-b-c, along with the experimental observations or earlier calculations.

In the case of NaCl, our predictions (solid line) were compared with experimental measurements (squares) provided by Akella et al. [50], as a function of pressure. The agreement between the theoretical results and measurements was excellent, and the average absolute discrepancy, that is,

$$< |\Delta T\%| > = \frac{1}{N}\sum_{j=1}^{N} \frac{\left|T(P_j)_{m,Theo} - T(P_j)_{m,Obs}\right|}{\left(\frac{T(P_j)_{m,Theo}+T(P_j)_{m,Obs}}{2}\right)} \times 100 \quad (49)$$

was less than 0.2 %, with a maximum deviation among the addends in (49) of 0.4 % (the average Clapeyron slope, $<dP/dT>$, was 0.019 *versus* 0.019 GPa/K, calculated and observed, respectively). The figure of merit defined at (49) was chosen to account for the heterogeneous nature of the involved data (in the case of stishovite, observations and earlier calculations are concomitantly employed for a comparison with our results) and the large estimates of the experimental uncertainties. The $\Delta H/\Delta V$ values for melting obtained using Eq. (36) range from 4.8 to 28.6 GPa, and they are the largest observed associated with $K_T \rightarrow 0$ (*P*-range: room pressure-6.5 GPa; *T*-range: 1074–1830 K), to be compared with ~2.7 GPa for the B1-B2 solid-solid phase transition by Li and Jeanloz (1987) [55], over the *P-T* range 23–27 GPa and 300–670 K. At room pressure, $K_T \rightarrow 0$ yields 1074, *versus* 1074 [50] and 1097 K [56] by measurements, and 1153 K by the quasi-harmonic model [28]. The degree of sensitivity of the melting curve to the *P-V-T* EoS model that is used to treat data was tested. In particular, the generalized Birch EoS (BM) by Belonoshko and Dubrovinsky [57] (dot-dashed line) and Mie-Grünesen model (MG) using the *P*-function of Aizawa and Yoneda [49] (dashed line) were fitted to the *P-V-T* data obtained by quantum simulations. The two EoS models provide results close to each other, though distinguishable, in the low pressure and high pressure ranges. The former EoS yields a melting curve closer to the experimental observations in the low compression regime ($\Delta V/V_0 < 1$ %) than the latter, whereas the reverse takes place in the high compression regime ($\Delta V/V_0 > 2$ %). This aspect can also justify the satisfactory behaviour of the Mie-Grüneisen model in fitting *P-V-T* data and predicting T_m for stishovite and perovskite, both high pressure phases, as it will be stated below. Yet it must be stressed how such EoS models were developed foremost for the high pressure-high temperature regime of a given phase, which is assumed stable. In the light of this, the discrepancies of BM *versus* MG, and of both models *versus* observations, can be explained by the fact that these models are applied in this study beyond their natural limits. All this suggests that, on the one hand, equations of state are able to carry information referring to melting and, on the other hand, care is to be paid in extrapolating a melting curve by EoS models.

In the case of $SiO_{2,st}$, the measurements from Shen and Lazor [58] and Zhang et al. [59], along with the theoretical results obtained by Luo et al. [60] and Belonoshko and Dubrovinsky [52], were used as "observations" for a comparison with our calculations, relying on the parametric model from Wang et al. [46]. $< |\Delta T\%| >$ is 5.8 %, and the largest absolute discrepancy among addends in (48) amounts to 13.8 % (Clapeyron slope, dP/dT, is 0.018 *versus* 0.020 GPa/K, calculated and observed, respectively). The $\Delta H/\Delta V$ figures of melting are spread over the interval 50–106 GPa, *versus* those of the stishovite-coesite equilibrium curve ranging in 3.8–5.8 GPa, by Ono et al. [61], whose measurements were performed at 6–11 GPa and 1200–1800 K.

For $MgSiO_3$, using the experimental data by Shen and Lazor [58], $< |\Delta T\%| >$ is 3.2 %, with a maximum absolute discrepancy of 6.2 % (Clapeyron slope, dP/dT, is 0.023 *versus* 0.020 GPa/K, calculated and observed, respectively). $\Delta H/\Delta V$ is forecast to range between 53 and 93 GPa *versus* 45 and 79 GPa from measurements performed over an experimental *P-T* range of 7–34 GPa and 2300–4050 K. A further comparison can be carried out between our $T_d(P_d)$ curve and that reported by Belonoshko et al. [62] determined by *ab-initio* molecular dynamics, complemented with semi-empirical potentials. Average agreements of 5.9 and 8.2 % were observed (using the discrepancy and absolute discrepancy for the former and latter figure of merit, respectively) in the interval of 25–90 GPa. The percentage deviation (Δ) between the present results and those of the aforementioned authors increases linearly with pressure, following a trend expressed by $\Delta = 0.3991 \times P$ (GPa)-17.08. This implies an agreement of approximately ±5 % up to ~60 GPa, and a progressively increasing positive divergence at higher pressures.

The average discrepancy figures between T_d (modelling) and T_m (available experimental data; for stishovite, some theoretical data are also included), that is,

$$< \Delta T\% > = \frac{1}{N}\sum_{j=1}^{N} \frac{\left(T(P_j)_{m,Theo} - T(P_j)_{m,Obs}\right)}{\left(\frac{T(P_j)_{m,Theo}+T(P_j)_{m,Obs}}{2}\right)} \times 100 \quad (50)$$

were −0.13, −3.6 and −0.3 % for NaCl, $SiO_{2,st}$ and $MgSiO_3$, respectively. In comparison with the $< |\Delta T\%| >$ discussed above, $< \Delta T\% >$ indicates that, on the one hand, compensation occurs between underestimates and overestimates and, on the other hand, the model relying on the *locus* of $K_T = 0$ leads to a slight underestimation of T_m. Note that the deviations of the calculations from the experimental data do not seem to show any systematic trend ($SiO_{2,st}$ and $MgSiO_3$ exhibit an opposite behaviour with pressure) but a slight overall prevalence for $T_d < T_m$ (Fig. 4a–c). We believe that the excellent agreement in the case of NaCl (Fig. 4a) is due to the fact that simulated data were employed to reconstruct the $T_d(P_d)$ curve, thus reducing the degree of uncertainty associated with the use of the experimental *P-V-T EoSs*, whose precision is high when the solid phase is fully stable, as stated above. Moreover, in the case of stishovite and perovskite, the actual complexity of measuring the melting curves should be considered, as both phases are stable only in the high-pressure regime.

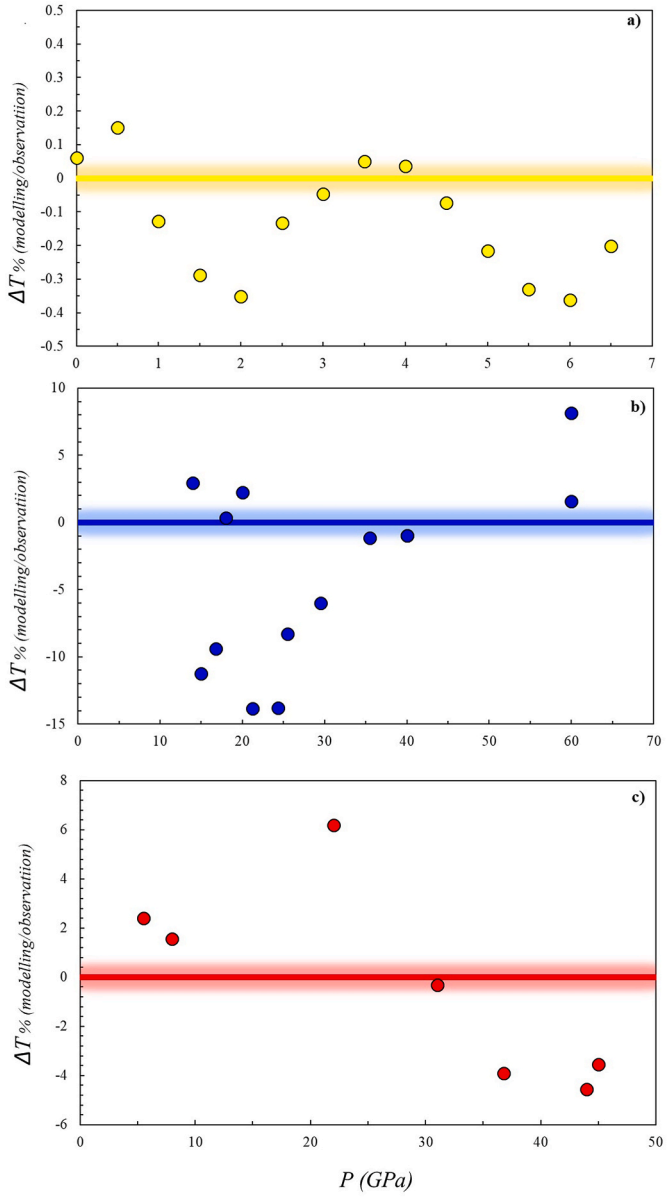

Fig. 4. Melting temperatures resulting by our modelling are compared with available literature data ($\Delta T\%$) calculated as $(T_{m,Theo}\text{-}T_{m,Obs})/(T_{m,Theo} + T_{m,Obs}) \times 200$ (i.e. the addends of (50)). Experimental data ($T_{m,Obs}$) as reported in Fig. 3. $T_{m,Theo}$ is estimated by T_d. (**a**) halite, (**b**) stishovite and (**c**) Mg-perovskite.

A further analysis of the phenomenology under investigation is significant in the context of the Negative Thermal Expansion (NTE) systems that are motivating an ever-increasing attention [63]. The model developed by Liu et al. [64] for NTE can be explored for the present case. The quoted authors claim that NTE is explainable in terms of the statistical occurrence of two phases separated by an equilibrium boundary with Clapeyron slope $dT/dP < 0$. Following their approach, a Vegard-like approximation can be used to model compressibility (strain energy of incorporation of one phase into the other is set aside), i.e. $\beta = 1/K_T$,

$$\beta V = -\left(\frac{\partial V}{\partial P}\right)_T = -\left(\frac{\partial[V_a f_a + V_b(1-f_a)]}{\partial P}\right)_T = \left(\frac{\partial f_a}{\partial P}\right)_T (V_b - V_a) + f_a(V_a\beta_a - V_b\beta_b) + V_b\beta_b = \left(\frac{\partial f_a}{\partial P}\right)_T (V_b - V_a) + V_b\beta_b(1-f_a) + V_a\beta_a f_a \quad (51)$$

where f_j is the probability to have the jth-phase (structure configuration), and can be written as follows

$$f_a = \frac{e^{-\Delta G/RT}}{1 + e^{-\Delta G/RT}} = \frac{1}{e^{\Delta G/RT} + 1}$$

$$f_b = \frac{1}{1 + e^{-\Delta G/RT}}$$

$$\left(\frac{\partial f_a}{\partial P}\right)_T = \frac{e^{\Delta G/RT}}{(e^{\Delta G/RT} + 1)^2} \frac{V_a - V_b}{RT}$$

taking $\Delta G = G_a - G_b$. The condition $K_T \to 0^+$ that is associated with $\beta \to +\infty$ was analysed. For a divergence of compressibility to be achieved in Eq. (51), it is required that either $\beta_a f_a \to +\infty$, or $\beta_b(1\text{-}f_a) \to +\infty$. Assuming that β_a and β_b do not diverge both, the divergence of compressibility looks like a phenomenon that can be related to the elastic behaviour of *one* phase (*a* or *b*, stable or metastable, respectively), rather than to the need of a statistical coexistence and interplay of stable and metastable configurations, like the mechanism proposed to account for NTE.

4. Conclusions

A vanishing isothermal bulk modulus K_T at $(P,V,T)_d$ is univocally associated with the occurrence of a degenerate critical point of the ΔG_{irrev} function, which represents the Gibbs energy change taking place in an irreversible transformation from the off-equilibrium point $(P_d,V_d/2+\delta V,T_d) + (P_d,V_d/2\text{-}\delta V,T_d)$ to $(P,V,T)_d$, at equilibrium. On the one hand, such a condition is related to the approaching instability of the system, as predicted by the catastrophe theory of Thom, and, on the other hand, it is related to the violation of the thermodynamic inequality for irreversible transformations that requires $\Delta G_{irrev} < 0$ and $\Delta S_{irrev} > 0$, at any order of expansion with respect to a deviation from equilibrium ($\pm\delta V$). This makes it impossible for the system to preserve a stable equilibrium, at $K_T = 0$ ("limit of stability"). Therefore, this is the precondition to a transformation into a new phase. The study of the *P-T locus* of $K_T = 0$ allows the characterization of the transformation in terms of T_d and $\Delta H/\Delta V$, the latter *via* the Claperyron slope, thus providing a way to locate among the possible manifolds the one that is the best candidate for melting. Three case studies are discussed: halite (NaCl), stishovite ($SiO_{2,st}$), and perovskite ($MgSiO_3$). Calculations were carried out by quantum modelling for halite and through semi-empirical *P-V-T EoS* parametric models for stishovite and perovskite. The agreement in terms of the absolute deviation of the melting curves between the calculations and observations ranges between 0.2 % (halite) and 5.8 % (stishovite), and the largest discrepancy of the predicted Clapeyron slope from the experimental dP/dT is within 14 %. The largest average discrepancy, in absolute value, between the theoretical results and experimental data ($< \Delta T\% >$) is −3.6 %. The present comparison between the predictions and observations must be performed with due care because of the comparatively small number of crystals whose *P-T* melting curves were analysed in detail. Moreover, in the case of NaCl the sensitivity of the predicted melting temperature curve to the EoS model was considered, using the Birch *versus* Mie-Grüneisen equations of state. It was observed that they lead to discrepancies, in the low and high pressure regimes. Although a vanishing isothermal bulk modulus does not ultimately provide a theoretical constraint to melting, yet $K_T \to 0$ implies instability *via* catastrophe theory and thermodynamic

inequality violation. Moreover, $\lim_{T\to T_m}\alpha = \infty$ is commonly recognized to occur at approaching fusion, and implies $K_T \to 0$. Altogether, the agreement between our modelling and observations is satisfactory. All this makes us confident that $K_T = 0$, at the highest temperature and largest $\Delta H/\Delta V$, allows the determination of a T_d that is a sound approximation of the physical T_m. Yet, the mechanism for $K_T \to 0$ seems to be less restrictive than that of NTE systems, insofar as the Vegard-like model discussed in the text holds. It is worth stressing that the comparative simplicity of application of the catastrophe theory, in combination with its solid mathematical basis, makes it an effective "universal" tool for the investigation of the stability of systems in the frame of the one-phase approach, as substantiated by the thermodynamic analysis of irreversible transformations involving solids in the *P-V-T* space, and not restricted to melting only.

CRediT authorship contribution statement

Marcello Merli: Writing – review & editing, Software, Methodology, Data curation, Conceptualization. **Costanza Bonadiman:** Writing – review & editing, Writing – original draft, Funding acquisition, Conceptualization. **Alessandro Pavese:** Writing – review & editing, Writing – original draft, Validation, Supervision, Funding acquisition, Formal analysis, Conceptualization.

Funding

This theoretical study was supported by the University of Turin (PASL_RILO-24_01; AP) and the University of Ferrara (2022_PRA. NB_FST_BC; CB). We acknowledge University of Palermo (FFR_D14_MERLI_2021;MM) for the computing resources assigned to this project.

Declaration of competing interest

The authors declare that they have no known competing financial interests or personal relationships that could have appeared to influence the work reported in this paper.

Acknowledgements

The authors acknowledge the support of the University of Palermo, University of Ferrara and University of Torino for the present work. The authors are grateful to the three anonymous Reviewers and the Chief Editor for suggestions and comments that promoted a stimulating discussion, which vastly benefitted the manuscript. The authors are also grateful to Barbara Galassi and Steve Deforie for the language editing.

Data availability

Data will be made available on request.

References

[1] R. Thom, Stuctural Stability and Morphogenesis, Benjamin-Addison-Wesley, New York, 1975.
[2] J. Milnor, Morse Theory, Princeton University Press, 1963. ISBN 0-691-08008-9.
[3] V.L. Arnol'd, Catastrophe Theory, 2nd-edition, Springer-Verlag, Berlin, 1986.
[4] I. Stewart, Applications of catastrophe theory to the physical sciences, Phys. Nonlinear Phenom. 2 (2) (1981) 245–305, https://doi.org/10.1016/0167-2789(81)90012-9.
[5] T. Poston, I. Stewart, Catastrophe theory and its applications. Series: Dover Books on Mathematics, Dover Publications, 1996. ISBN: 9780486692715.
[6] M. Merli, A. Pavese, Electron-density critical points analysis and catastrophe theory to forecast structure instability in periodic solids, Acta Crystallogr. A74 (2018) 102–111, https://doi.org/10.1107/S2053273317018381.
[7] M. Merli, A. Pavese, Melting temperature prediction by thermoelastic instability: an ab initio modelling, for periclase (MgO), Calphad 73 (2021) 102259, https://doi.org/10.1016/j.calphad.2021.102259.
[8] G. de With, Melting is well-known, but is it also well-understood? Chem. Rev. 123 (23) (2023) 13713–13795, https://doi.org/10.1021/acs.chemrev.3c00489.
[9] V. Gharakhanyan, L.J. Wirth, J.A. Garrido Torres, E. Eisenberg, T. Wang, D. R. Trinkle, S. Chatterjee, A. Urban, Discovering melting temperature prediction models of inorganic solids by combining supervised and unsupervised learning, J. Chem. Phys. 28 160 (20) (2024) 204112, https://doi.org/10.1063/5.0207033.
[10] G.J. Ackland, H. Zong, V.N. Robinson, S. Scandolo, A. Herman, Two-state model for critical points and the negative slope of the melting curve, Phys. Rev. B 104 (2021) 054120. https://link.aps.org/doi/10.1103/PhysRevB.104.054120.
[11] Li-F. Zhu, B. Grabowski, J. Neugebauer, Efficient approach to compute melting properties fully from ab initio with application to Cu, Phys. Rev. B 96 (2017) 224202, https://doi.org/10.1103/PhysRevB.96.224202.
[12] A.B. Belonoshko, N.V. Skorodumova, A. Rosengren, B. Johansson, Melting and critical superheating, Phys. Rev. B 73 (2006) 012201. https://link.aps.org/doi/10.1103/PhysRevB.73.012201.
[13] A.B. Belonoshko, L. Burakovsky, S.P. Chen, B. Johansson, A.S. Mikhaylushkin, D. L. Preston, S.I. Simak, D.C. Swift, Molybdenum at high pressure and temperature: melting from another solid phase, Phys. Rev. Lett. 100 (2008) 135701. https://link.aps.org/doi/10.1103/PhysRevLett.100.135701.
[14] A.B. Belonoshko, Molecular dynamics of silica at high pressures: equation of state, structure, and phase transitions, Geochim .et Cosmochim. Acta 58 (6) (1994) 1557–1566.
[15] A.J. C Ladd, L. V Woodcock, Interfacial and co-existence properties of the Lennard-Jones system at the triple point, Mol. Phys. 36 (2) (1978) 611–619, https://doi.org/10.1080/00268977800101791.
[16] C. Chakravarty, R.M. Lynden- Bell, Landau free energy curves for melting of quantum solids, J. Chem. Phys. 113 (20) (2000) 9239–9247, https://doi.org/10.1063/1.1316105.
[17] K. Trachenko, Theory of melting lines, Phys. Rev. E 109 (2024) 034122, https://doi.org/10.1103/PhysRevE.109.034122.
[18] F.A. Lindemann, The calculation of molecular vibration frequencies, Phys. Z. 11 (1910) 609–612.
[19] J.J. Gilvarry, The Lindemann and grüneisen laws, Phys. Rev. 102 (1956) 308–316, https://doi.org/10.1103/PhysRev.102.317.
[20] F. Guinea, J.H. Rose, J.R. Smith, J. Ferrante, Scaling relations in the equation of state, thermal expansion, and melting of metals, Appl. Phys. Lett. 1 44 (1) (1984) 53–55, https://doi.org/10.1063/1.94549.
[21] F. D Stacey, R. D Irvine, Theory of melting: thermodynamic basis of Lindemann's law, Aust. J. Phys. 30 (1977) 631–640, https://doi.org/10.1071/PH770631.
[22] J. Zhang, H. Zhang, J.F. Douglas, A closer examination of the nature of atomic motion in the interfacial region of crystals upon approaching melting, J. Chem. Phys. 160 (2024) 114506, https://doi.org/10.1063/5.0197386.
[23] K.F. Herzfeld, M. Goeppert Mayer, On the theory of fusion, Phys. Rev. 46 (1934) 995–1001, https://doi.org/10.1103/PhysRev.46.995, 1934.
[24] M. Born, Thermodynamics of crystals and melting, J. Chem. Phys. 7 (8) (1939) 591–603, https://doi.org/10.1063/1.1750497. ISSN 0021-9606.
[25] Y. Ida, Theory of melting based on lattice instability, Phys. Rev. 187 (1969) 951–958, https://doi.org/10.1103/PhysRev.187.951.
[26] L.L. Boyer, Theory of melting based on lattice instability, Phase Transitions 5 (1985) 1–48, https://doi.org/10.1080/01411598508219144.
[27] F.J. Owens, The thermo-elastic instability model of melting of alkali halides in the Debye approximation, Phase Transitions 91 (5) (2018) 503–508, https://doi.org/10.1080/01411594.2018.1432052.
[28] R. M Digilov and H. Abramovich, "Temperature variation of the isothermal bulk modulus in solids: Thermo-elastic instability and melting". J. Appl. Phys. 125 065104. https://doi.org/10.1063/1.5078722.
[29] H.B. Callen, Thermodynamics, John Wiley & Sons Inc, 1960.
[30] R. Gilmore, "*Catastrophe Theory*". (Encyclopedia of Applied Physics, John Wiley & Sons Ltd, 2003.
[31] J. C Tolédano, P. Tolédano, The Landau theory of phase transitions, World Scientific Lecture Notes in Physics 3 (1987).
[32] J. Rumble, Handbook of Chemistry and Physics, *104*, CRC Press, 2023. ISBN 9781032121710.
[33] V.M. Glazov, O.D. Shchelikov, Volume changes during melting and heating of silicon and germanium melts, High Temp. 38 (2000) 405–412, https://doi.org/10.1007/BF02756000.
[34] L.J. Wittenberg, R. DeWitt, Volume contraction during melting; emphasis on lanthanide and actinide metals, J. Chem. Phys. 56 (9) (1972) 4526–4533, https://doi.org/10.1063/1.1677899.
[35] Zi-K. Liu, Computational thermodynamics and its applications, Acta Mater. 200 (2020) 745–792, https://doi.org/10.1016/j.actamat.2020.08.008.
[36] Zi-K. Liu, Quantitative predictive theories through integrating quantum, statistical, equilibrium, and nonequilibrium thermodynamics, J. Phys. Condens. Matter 36 (2024) 343003, https://doi.org/10.1088/1361-648X/ad4762.
[37] V.A. Drebushchak, Thermal expansion of solids: review on theories, J.Therm. An. and Calorim. 142 (2020) 1097–1113, https://doi.org/10.1007/s10973-020-09370-y.
[38] R. J Angel, M. Alvaro, R. Miletich, F. Nestola, A simple and generalised P–T–V EoS for continuous phase transitions, implemented in EosFit and applied to quartz, Contrib. Mineral. Petrol. 172 (2017) 29, https://doi.org/10.1007/s00410-017-1349-x.
[39] J. McConnell, C. Mccammon, R. Angel, F. Seifert, The nature of the incommensurate structure in åkermanite, $Ca_2MgSi_2O_7$, and the character of its transformation from the normal structure, Z. für Kristallogr. - Cryst. Mater. 215 (11) (2000) 669–677, https://doi.org/10.1524/zkri.2000.215.11.669.
[40] R. Dovesi, A. Erba, R. Orlando, C.M. Zicovich-Wilson, B. Civalleri, L. Maschio, M. Rérat, S. Casassa, J. Baima, S. Salustro, B. Kirtman, Quantum-mechanical

condensed matter simulations with CRYSTAL, WIREs Comp. Mol. Sc. 1360 (2018), https://doi.org/10.1002/wcms.1360, 2018.
[41] Y. Zhao, D.G. Truhlar, Construction of a generalized gradient approximation by restoring the density-gradient expansion and enforcing a tight Lieb–Oxford bound, J. Chem. Phys. 128 (2008) 184109, https://doi.org/10.1063/1.2912068.
[42] J.P. Perdew, K. Burke, Y. Wang, Generalized gradient approximation for the exchange-correlation hole of a many-electron system, Phys. Rev. B 54 (1966) 16534–16537, https://doi.org/10.1103/physrevb.54.16533.
[43] M. Towler, CRYSTAL Resources Page, Theory of Condensed Matter, 2015. http://www.tcm.phy.cam.ac.uk/~mdt26/crystal.html.
[44] G. Sophia, P. Baranek, C. Sarrazin, M. Rerat, R. Dovesi, First-principles study of the mechanisms of the pressure-induced dielectric anomalies in ferroelectric perovskites, Phase Transitions 81 (2013) 1069–1084.
[45] E. Aprà, M. Causà, M. Prencipe, R. Dovesi, V.R. Saunders, On the structural properties of NaCl. An *ab initio* study of the B1-B2 phase transition, J. Phys. Condens. Matter 5 (1993) 2969–2976.
[46] A. Otero-de-la-Roza, D. Abbasi-Pérez, V. Luaña V, Gibbs2: a new version of the quasi-harmonic model code. II. Models for solid-state thermodynamics, features and implementation, Comput. Phys. Commun. 182 (2011) 2232–2248.
[47] Z. Wu, R. Wentzcovich R, Effective semiempirical ansatz for computing anharmonic free energies, Phys.Review B 79 (2009) 104304, https://doi.org/10.1103/PhysRevB.79.104304.
[48] F. Wang, Y. Tange, T. Irifune, K. Funakoshi, P-V-T equation of state of stishovite up to mid-lower mantle conditions, J. Geophys. Res. 117 (2012) B06209, https://doi.org/10.1029/2011JB009100.
[49] Y. Aizawa, A. Yoneda, P-V-T equation of state of $MgSiO_3$ perovskite and MgO periclase: implication for lower mantle composition, Phys. Earth Planet. In. 155 (2006) 87–95.
[50] J. Akella, S.N. Vaidya, G:C: Kennedy, Melting of sodium chloride at pressures to 65 kbar, Phys. Rev. 185 (1969) 1135–1140.
[51] R.A. Robie, B.S. Hemingway, J.R. Fisher, Thermodynamic Properties of Minerals and Related Substances at 298.15 K and 1 Bar (105 Pascals) Pressure and at Higher Temperatures vol. 1452, Geological Survey Bullettin, Washington, DC (USA), 1978.
[52] A.B. Belonoshko, L.S. Dubrovinsky, Molecular dynamics of stishovite melting, Geochim.et Cosmochim. Acta 59 (1995) 1883–1889.
[53] M. Millot, N. Dubrovinskaia, A.A. Černok, S. Blaha, L. Dubrovinsky, D.G. Braun, P. M. Celliers, G.W. Collins, J.H. Eggert, R. Jeanloz R, Shock compression of stishovite and melting of silica at planetary interior conditions, Science 347 (2015) 418–420.
[54] C.P. Di Paola, J. Brodholt, Modeling the melting of multicomponent systems: the case of $MgSiO_3$ perovskite under lower mantle conditions, Sci. Rep. 6 (2016) 29830, https://doi.org/10.1038/srep29830.
[55] X. Li, R. Jeanloz, Measurement of the B1-B2 transition pressure in NaC1 at high temperatures, Phys. Rev. B 36 (1987) 474–479. https://DOI:10.1103/PHYSREVB.36.474.
[56] J. Emsley, The Elements, Oxford University Press, Oxford, 1989.
[57] A.B. Belonoshko, L.S. Dubrovinsky, Molecular dynamics of NaCl (B1 and B2) and MgO (B1) melting: two-phase simulation, Am. Mineral. 81 (1996) 303–316, https://doi.org/10.2138/am-1996-3-404.
[58] G. Shen, P. Lazor P, Measurement of melting temperatures of some minerals under lower mantle pressures, J. Geophys. Res. 100 (1995), https://doi.org/10.1029/95JB01864, 17699-1713.
[59] J. Zhang, R.C. Liebermann, T. Gasparik, C.T. Herzberg, Melting and subsolidus relations of SiO_2 at 9-14 GPa, J. Geophys. Res. 98 (1993) 19785–19793, https://doi.org/10.1029/93JB02218.
[60] S. Luo, T. Cagin, A. Strachan, W.A. Goddard, T.J. Ahrens, Molecular dynamics modeling of stishovite, Earth Planet Sci. Lett. 202 (2002) 147–157, https://doi.org/10.1016/S0012-821X(02)00749-5.
[61] S. Ono, T. Kikiîegawa, Y. Higo, Y. Tange, Precise determination of the phase boundary between coesite and stishovite in SiO_2, Phys. Earth Planet. In. 264 (2017) 1–6, https://doi.org/10.1016/j.pepi.2017.01.003.
[62] A.B. Belonoshko, N.V. Skorodumova, A. Rosengren, R. Ahuja, B. Johansson, L. Burakovsky, D.L. Preston, High-pressure melting of $MgSiO_3$, Phys. Rev. Lett. 94 (2005) 195701, https://doi.org/10.1103/PhysRevLett.94.195701.
[63] N. Shi, Y. Song, X. Xing, J. Chen, Negative thermal expansion in framework structure materials, Coord. Chem. Rev. 449 (2021) 214204, https://doi.org/10.1016/j.ccr.2021.214204.
[64] Zi-K. Liu, Y. Wang, Shun-L. Shang, Origin of negative thermal expansion phenomenon in solids, Scripta Mater. 65 (8) (2011) 664–667, https://doi.org/10.1016/j.scriptamat.2011.07.001.